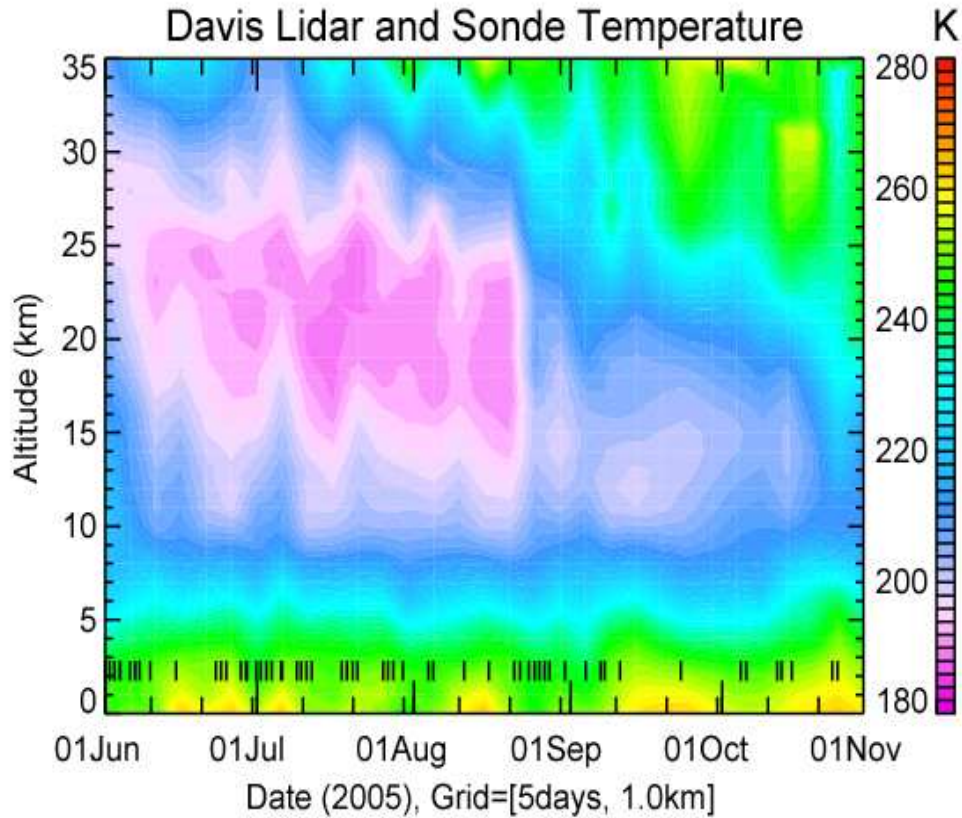


BMRC Research Letter No 4.



Contents

<i>The Impact Of Recent Events On Our Understanding Of Tropical Cyclones And Climate Change</i>	2-10
<i>Ozone and temperature above Davis, Antarctica, during the austral winter and spring of 2005</i>	11-15
<i>An Examination of Dewpoint Biases Introduced by Different Instrumentation</i>	16-26
<i>Meridional transport of low-latitude stratospheric air to the Antarctic region</i>	27-33
<i>UV Index for Sun-Safety</i>	34-35

Editors

L.Deschamp, G.Roff and A.Hollis

email:A.Hollis@bom.gov.au

The Impact Of Recent Events On Our Understanding Of Tropical Cyclones And Climate Change

Jeffrey D. Kepert

Bureau of Meteorology Research Centre

Email: j.kepert@bom.gov.au

Abstract.

This letter attempts to briefly bring together some of the issues pertaining to tropical cyclones and climate change, in the light of recent events. Here, “recent events” includes Hurricanes Katrina and Rita, the very active 2004 and 2005 seasons in the North Atlantic, and the publications by Webster et al. (2005) and Emanuel (2005a) on tropical cyclone intensity trends, which have collectively provoked considerable media and political interest. The purpose is to be brief rather than detailed, and to help the Bureau to present a consistent and scientifically reasonable view. Walsh (2004) gives a recent thorough review, which is recommended for those wanting more detail.

What does Emanuel (2005a) tell us?

Emanuel (2005a) studies tropical cyclone best-track data for the North Atlantic since 1943. His main index of activity is the power dissipation index (PDI), which is the integral of the maximum wind speed cubed over the storm lifecycle. His figures show a small decrease in the annual total of this quantity until the 1980s, followed by an increasing trend that became very rapid around 1995. These changes are claimed to be highly correlated with SST changes. For the NW Pacific, a similar increase occurred in the late 1980's. These trends reflect increases in both storm duration (up by about 60%) and intensity (annual mean peak wind speed cubed up by about 50%¹).

Emanuel examines whether these changes can be attributed to increased SST, to changes in the maximum potential intensity² (MPI) and to changes in the mean tropospheric shear. While changes in each of these factors are consistent with the direction of the observed change, the first two explain only a small part of the magnitude of the change, while the shear changes are very small and explain almost none of it.

Emanuel's results in the northwest Pacific are in apparent contradiction with the work of Chan and Liu (2004), who find a weak negative correlation between SST and typhoon activity in that basin. This is a result of the influence of ENSO on these two quantities: El Nino years have high typhoon activity in the northwest Pacific. Chan and Liu explain this association between El Nino and typhoon activity in terms of

¹ Emanuel (2005a) incorrectly states that the annual peak mean wind speed, rather than its cube, has increased by 50%. The 50% increase in the cube is correct (K.A. Emanuel, personal communication, 2006) and corresponds to an increase in the mean of about 15%.

² MPI theories (e.g. Emanuel 1995, Holland 1997) aim to predict the maximum intensity a tropical cyclone can reach in a given thermodynamic environment, in the absence of intensity-limiting factors such as environmental vertical shear, landfall, or movement over cooler water. MPI depends on sea surface temperature (warmer gives higher MPI), and also on other factors such as the upper tropospheric temperature (warmer gives lower MPI).

dynamical and thermodynamic factors including low-level relative vorticity, vertical wind shear and moist static energy, which dominate any local SST signal. The reason that Emanuel found an opposite SST-typhoon relationship to Chan and Liu is probably that he applied a time-filter, which removes or weakens the ENSO signal.

Landsea (2005) has criticised Emanuel's study on several grounds. In particular, the visual impact of the recent increase is exaggerated in the North Atlantic by the inclusion of unfiltered data for the last two years³. Intensity data prior to 1969 had a downwards bias correction applied after Landsea (1993). This is claimed to have been misapplied and to be too large: if it is not applied, the pre-1960 PDI is comparable to that post-1995. Landsea (2005) presents figures comparing these bias corrections for the North Atlantic, showing a significant change in the pre-1969 storms. Note also that Emanuel's use of a speed-cubed relationship increases the magnitude of any change, real or otherwise.

Emanuel (2005b) has responded to these comments. The unfiltered endpoints are acknowledged, as is the excessive bias correction. A graph with a new bias correction is presented, for the combined activity in the West Pacific, East Pacific and North Atlantic basins, which shows an upwards trend from about 1980, but with a marked downwards kick in the late 1990's. This web page includes a stronger statement than the original Nature article: "This work implies that global tropical cyclone activity is responding in a rather large way to global warming."

What do Webster et al. (2005) tell us?

Webster et al. (2005) consider tropical cyclone best-track data from the satellite era (1970 - 2004). Their main findings are that, over this period,

- SST has increased in most TC-prone ocean basins by about 0.5 K.
- The annual total global numbers of TCs and intense TCs have not changed.
- The annual total global number of TC days and intense TC days has not changed, although the number of intense TC days reached a maximum near 1995 and has since declined.
- These "global" conclusions apply in each basin, except the North Atlantic, where there is an increasing trend in frequency and duration. However, a simple attribution of the North Atlantic trend to local SST is not supported, as a similar relationship is absent in the other basins.
- The number of storms in the most intense categories (4 and 5) has nearly doubled over the period, as has the percentage of storms in these categories. However, there has been no change in the intensity of the most intense storms; the change consists of a skewing, rather than a shift, of the frequency distribution of observed intensity to the right. This change is broadly consistent with Emanuel's 50% increase in the annual mean peak wind speed.

Note that this study omitted storms that formed in the Australian region, because a significant proportion of these have their intensity constrained by landfall.

³ Note that Emanuel's study included the 2004 North Atlantic season, but not the very active 2005.

Can these changes be due to natural variability?

Goldenberg et al. (2001) and others have shown that there is a multidecadal cycle in hurricane activity in the North Atlantic, with active periods from 1920's - 1960, inactive from 1960 - 1994, then a return to the current active phase. A somewhat similar cycle is present in the landfall statistics. The cause of the cycle is at present unknown. One hypothesis, discussed by Goldenberg et al., is that it is related to a cycle in the Atlantic thermohaline circulation, with active hurricane periods corresponding to a strong thermohaline circulation. However, measurements (Bryden et al. 2005) show a recent decrease in the circulation, which is probably sufficient to eliminate this hypothesis.

The existence of this cycle implies that the increase in frequency of intense storms in the North Atlantic noted by Emanuel (2005a) and by Webster et al. (2005) since 1995 is partly or wholly due to natural causes. It is not clear why Emanuel does not detect the pre-1960 maximum in his data, but it may be that Goldenberg et al. looked at the number of intense hurricanes, while Emanuel's measure includes all storms and the intensity and duration. Also, recall that Landsea (2005) argues that Emanuel misses the earlier peak because of the use of an excessively large bias correction to that period. Note that Webster et al. do not consider data before 1970.

Given the uncertainties in the historical best-track database (next section), one could question whether Goldenberg et al.'s results are possibly an artefact of these changes. However, since a similar signal is present in U.S. landfalling storms, and as the population density has been sufficient since about 1900 to detect all such events, the evidence for this sequence of active and inactive periods seems solid.

Are the best-track databases suitable for this sort of study?

Intensity estimation methods have changed, even in the satellite era, due to the changes in satellite coverage (frequency, resolution and spectral, not to mention scatterometers) and analysis techniques. Satellite intensity estimates are usually based on the "Dvorak technique", a semi-objective pattern-recognition technique originally developed in the 1970's to use visible imagery, and extended in the 1980's to infrared. It has also been subject to gradual evolution in time, and there are known inter-basin differences (see Velden et al. 2005 for a historical review and discussion of these issues).

For aircraft reconnaissance in the North Atlantic, recent changes include the GPS dropsonde (1998), new aircraft-surface wind speed adjustment methods (2001), and the step-frequency microwave radiometer (2003). Aircraft in recent years tend to fly higher than in the early years (which probably affects surface wind estimation), and the aircraft wind speed measurement technology changed around 1980. An illustration of the impact of these changes is that reanalysis of Hurricane Andrew (1992) in 2002, using more recent ideas about data interpretation, changed the intensity at landfall from category 4 to 5 on the Saffir-Simpson scale (Landsea et al. 2004).

Before the satellite era a high degree of confidence is clearly very difficult to achieve, particularly for weak or small storms, or those far from land. Statements about

changes in the lifetime or number of storms are therefore particularly risky. While the aircraft reconnaissance era (post-1945) probably captured all significant North Atlantic storms, probably the full lifecycle of pre-satellite storms was not captured and this has reduced Emanuel's PDI measure in the early period.

Note that Emanuel adjusts the best-track data to attempt to overcome some of these difficulties, while Webster et al. use it "as is". A consistent reanalysis during the satellite era would improve confidence, but is a major undertaking.

What do other studies say about intensity change?

Maximum potential intensity (MPI) studies suggest a possible increase in the intensity of the most intense storms by up to about 10% by 2050 (Henderson-Sellers et al. 1998). They are inherently unable to make predictions about the behaviour of storms below their MPI. They emphasise that MPI depends on more than just SST; an increase in SST will lead to an increase in MPI if the atmosphere remains unchanged, but atmospheric changes could reduce or eliminate the effects of the SST change. While these simplified theories produce good agreement with observations, this is partly due to the tuning of several assumed constants within the theory.

Knutson and Tuleya (2004) use a range of climate model forcings to drive a higher resolution cyclone model, with a range of physical parameterisations, and obtain an intensity increase of 6% to 14% by 2080, consistent with earlier work discussed by Walsh (2004). This result is also consistent with MPI theories, since Knutson and Tuleya placed their storms in a uniform easterly environmental flow, which will usually allow a model storm to develop to close to its MPI; thus their results do not directly apply to less intense storms.

It is important to recognise that SST is only one of several factors that affect TC intensity. For instance, Knutson and Tuleya (2004, their Figure 11) give separate regressions between intensity and SST for their present-climate and 2xCO₂ scenarios. While each shows increasing intensity with increasing SST, the intensity for a given SST is lower in the 2xCO₂ calculations than for the present climate, because the 2xCO₂ scenarios included greater warming in the upper troposphere than below. This increases outflow temperature and thereby reduces cyclone intensity (Emanuel 1995, Holland 1997). Similarly, Chan and Liu (2004) show that annual typhoon activity in the northwest Pacific is related to El Nino through factors such as low-level vorticity, wind shear and moist static stability, rather than through local SST changes.

Knutson and Tuleya (2004) also discuss rainfall intensity changes, for which they predict rather larger percentage increases than for wind (on a per-storm basis); note that rainfall and flood risk are generally not well correlated with wind intensity. Groisman et al. (2004) analyse precipitation changes over the past century. They find no significant change in hurricane-related precipitation along the US coast over the past century, in spite of increases in total precipitation and in the frequency of very heavy non-hurricane precipitation. They decline to analyse changes in per-storm (as distinct from per-annum) hurricane precipitation.

Are the analyses of Emanuel and Webster et al. evidence of climate change?

Both papers are careful to not make this attribution, and to note that SST alone does not determine TC intensity.

Once a TC forms, it has a nearly equal probability of reaching any intensity up to its MPI (Emanuel 2000); over the past few decades, this distribution has become skewed, if the data are to be believed. But thermodynamic approaches, or modelling studies such as Knutson and Tuleya (2004) show an increase in MPI under greenhouse conditions. Webster et al. (2005) specifically state that there has been no increase in the annual maximum intensity. Thus there is a slight discrepancy between climate change predictions, and the observations. The discrepancy is slight because only a small amount of the predicted peak intensity change would have been realised at present, and detecting this in the presence of observational uncertainty is probably impossible.

Were Katrina, Rita and Wilma unprecedented events?

It is difficult to regard Katrina and Rita as unprecedented, while Wilma set a new record lowest central pressure for the North Atlantic basin following its extraordinarily rapid intensification. None was category-5 at landfall (there have previously been 3 such events in the United States). The 2005 season was however a record season on several counts: the most category-5 storms (3, previous record 2 in 1960 and 1961), the most hurricanes⁴ (15, previous record 12 in 1969), the most named storms (26, beating 21 in 1933) and the lowest central pressure (882 hPa in Hurricane Wilma)⁵. These records are certainly significant. However, without wishing to degrade this significance, but wanting to keep matters in perspective, a few of the season's storms were short-lived and/or spent their entire lives in remote parts of the Atlantic Ocean. It is likely that they would not have been detected, or had their intensity recognised, in the pre-satellite era.

Some reports have described Katrina as a "worst-case scenario". Note that Katrina had weakened to category-3 at landfall, and that Hurricane Camille of 1969 made landfall a little to the east as a category-5 storm. Things could have easily been worse. However, Katrina was arguably near worst-case as far as sea surface temperature goes, due to the conjunction of a very warm SST year with a proximate warm-core ring in the Gulf, and clearly worst-case in terms of the extraordinary vulnerability of New Orleans. On vulnerability, it is interesting to note that the Mississippi coast was devastated in Hurricane Camille (1969), and apparently was slow to rebuild until the mid-1980's, since when there has been rapid growth.

⁴ In the north Atlantic, a tropical cyclone is named when its maximum mean surface wind speed reaches 34 kt. A hurricane has maximum wind exceeding 64 kt, and a category-5 hurricane exceeds 136 kt.

⁵ These records are provisional, and current as of 6 Feb 2006. However the post-season best-track analysis is not yet complete and it is possible that further storms may have their intensity status changed.

Are Katrina, Rita and Wilma evidence of climate change?

One or two seasons tell us almost nothing on climatic time scales; however the SSTs are at or near record highs and there have been three category-5 storms in 2005. However, Katrina, Rita and Wilma reached this intensity at least as much because of the very favourable synoptic environment, as because of the high SST. So far, no relationship between the favourable synoptic conditions and climate change scenarios (or high SST) has been demonstrated. However, the near-record SST in the Gulf of Mexico and the presence of a steady warming trend likely indicates an anthropogenic component.

Multiple studies (in the refereed literature) of the rapid intensification of Hurricane Opal failed to agree on the cause (warm core ring or upper trough interaction); one pair of studies (Persing et al. 2002, Moller and Shapiro 2002) achieved opposite conclusions as to the importance of the upper trough interaction, based on analysis of the same model simulation. I suggest one can conclude from this is that it can be extraordinarily difficult to assign cause for the intensity change of a single storm, let alone several season's worth.

What might be the impact of an increase in the frequency of category 4 and 5 storms?

Properly designed, constructed and maintained structures should be able to largely withstand⁶ winds of this magnitude. Defending against storm surge (especially with waves superimposed) and riverine flooding is considerably more difficult and expensive. If surge and flood-prone areas were kept free of infrastructure, appropriate wind-engineering standards adhered to, and a high quality warning and response system maintained, a doubling of the frequency of the most severe storms could be argued to be not much more than an inconvenience, albeit a fairly severe one. These "ifs" clearly carry greater weight for less-developed nations than for Australia, where building codes and practices are relatively strict.

Note also that land use changes over the past few decades have increased vulnerability in many parts of the world by a much greater factor than the frequency shift noted by Webster et al. (2005). Pielke et al. (2005) strongly argue the case for increased vulnerability due to increased population, although one must be careful in reading their paper to note that they are comparing this change to the comparatively modest projections of TC change in the third IPCC report, and not to the much larger changes reported by Emanuel (2005a) and Webster et al. (2005). In considering anthropogenic climate change and vulnerability, one should also remember the potential for compounding changes – for example, the impact of an increase in TC activity will be greater if it is accompanied by a significant mean sea level rise.

⁶ By "largely withstand", I mean that the basic structure will remain intact. Minor external damage (e.g. to guttering, pergolas, and solar hot water services), and some water ingress, may occur. Also, structures subject to an intense debris stream, to falling trees, to inadequate maintenance or to poor construction practices can be expected to sustain more damage.

What are the implications for Australia?

Nicholls et al. (1998) found a decrease in TC numbers since 1970 for the Australian region, with a slight increase in the number of more intense storms. McBride (2004) notes a decrease in the numbers of both intense and all storms over a slightly longer period for the Australian region. He also notes a small increase in the number of very intense storms, but is not confident that this is real, given the changes in observations and intensity estimation techniques over this period. Both authors note that seasonal tropical cyclone activity in the Australian region is significantly modulated by ENSO. If climate change scenarios suggesting an increase in the frequency of El Nino are correct, this could result in a decreased cyclone frequency in the Australian region. Thus the strong ENSO modulation makes predicting future Australian region TC activity very difficult.

Tropical cyclones represent a major natural hazard to Australia and to many of our neighbours. For Australia, the increases in coastal vulnerability, in community expectations, and in meteorological knowledge emphasise the need for the Bureau to maintain an ongoing role in research into tropical cyclones, in order to support the further development of forecast and warning services on all time-scales. *An active research program is essential to maintain a world-class warning system and thereby limit the impact of these events.* The potential for climate change to impact upon tropical cyclones, and the need for accurate assessment of tropical cyclone risk even in the present climate, demonstrate the value of the existing best-track database and highlight the importance of future efforts to maintain, extend and quality control this resource.

Summary

Some studies show a recent increase in the frequency of the most intense storms. At present, it is not possible to attribute the cause of this to either anthropogenic climate change, or natural cycles. To do so, either way, would be to imply that we know a lot more than we do – probably both are having a role, and the question should be one of relative contributions. As the jury is out, it is arguably prudent to allow for the possibility of a human contribution to the reported change, at this stage. However, research is urgently needed to determine whether the apparent increase in activity is due to changes in observing systems. Research is also necessary to determine the extent to which multi-decadal cycles, similar to that in the North Atlantic, are present in other basins, not least because the presence of such oscillations makes the detection of trends more difficult. Such research requires long, high-quality datasets, which may not exist. It is also important to remember that the increase in vulnerability due to land use changes is in many locations substantially larger than the reported frequency change of intense TCs. Regardless of the cause, proper attention to mitigation can minimise the impact of such a change. However, a successful mitigation program requires a foundation of active research.

Acknowledgements

This is an update of an informal document originally prepared at the request of A/CSR. I acknowledge many fruitful discussions, as well as helpful comments on the original document. Contributors include Neville Nicholls, John McBride, David Jones, Chris Landsea, Kevin Walsh and Michael Foley. In

preparing this document, it has become clear that this is a contentious subject with some strongly held views. Positions include “entirely anthropogenic”, “entirely natural cycles” and “entirely changes in the observing system”. I believe none of these have been satisfactorily demonstrated, and so have attempted to give a balanced view and to emphasise the areas in which we are uncertain. I would welcome any scientific evidence to the contrary.

References

- Bryden, H.L., H.R. Longworth and S.A. Cunningham, 2005: Slowing of the Atlantic meridional overturning circulation at 25°N. *Nature*, **438**, 655 - 657. doi: 10.1038/nature04385.
- Chan, J.C.L. and K.S. Liu, 2004: Global warming and western north Pacific typhoon activity from an observational perspective. *J. Clim.*, **17**, 4590 - 4602.
- Emanuel, K.A., 1995: Sensitivity of tropical cyclones to surface exchange coefficients and a revised steady-state model incorporating eye dynamics. *J. Atmos. Sci.*, **52**, 3969-3976.
- Emanuel, K.A., 2000: A statistical analysis of tropical cyclone intensity. *Mon. Wea. Rev.*, **128**, 1139 - 1152.
- Emanuel, K.A., 2005a: Increasing destructiveness of tropical cyclones over the past 30 years. *Nature*, **436**, 686 - 688. doi: 10.1038/nature03906.
- Emanuel, K.A., 2005b: *Anthropogenic Effects on Tropical Cyclone Activity*. <http://wind.mit.edu/~emanuel/anthro2.htm>. Viewed on 16 December 2005.
- Goldenberg, S.B., C.W. Landsea, A.M. Mestas-Nunez and W.M. Gray, 2001: The recent increase in Atlantic hurricane activity: causes and implications. *Science*, **293**, 474 - 479.
- Groisman, P.Y. R.W. Knight, T.R. Karl, D.R. Easterling, B. Sun and J.H. Lawrimore, 2004: Contemporary changes of the hydrological cycle over the contiguous United States: Changes derived from in situ observations. *J. Hydrometeorol.*, **5**, 64 - 85.
- Henderson-Sellers, A., G. Berz, R. Elsberry, K. Emanuel, W.M. Gray, C. Landsea, G. Holland, J. Lighthill, S.-L. Shieh, P. Webster, and H. Zhang, 1998: Tropical cyclones and global climate change: A post-IPCC assessment. *Bull. Amer. Meteor. Soc.*, **79**, 19-38.
- Holland, G.J. 1997: The maximum potential of tropical cyclones. *J. Atmos. Sci.*, **54**, 2519-2541.
- Knutson, T.R. and R.E. Tuleya, 2004: Impact of CO₂-induced warming on simulated hurricane intensity and precipitation: sensitivity of the choice of climate model and convective parameterisation. *J. Clim.*, **17**, 3477 - 3495.
- Landsea, C. W., 1993: A climatology of intense (or major) Atlantic hurricanes. *Mon. Wea. Rev.*, **121**, 1703-1714.
- Landsea, C.W., J.L. Franklin, C.J. McAdie, J.L. Benen II, J.M. Gross, B.R. Jarvinen, J.P. Dunion and P.P. Dodge, 2004: A reanalysis of Hurricane Andrew's (1992) intensity. *Bull. Amer. Meteorol. Soc.*, **85**, 1699-1712.
- Landsea, C.W., 2005: Atlantic hurricanes and global warming. *Nature*, in press.
- McBride, J.L., 2004: Relationships between tropical cyclones and sea surface temperature in the Australian region: implications for anthropogenic climate change. Extended abstracts, *International Conference on Storms, AMOS 11th National Conference*. Australian Meteorological and Oceanographical Society, Brisbane, Australia, 5 - 9 July, 238 - 239.
- Moller, J.D. and L. Shapiro, 2002: Balanced contributions to the intensification of Hurricane Opal as diagnosed from a GFDL model forecast. *Mon. Wea. Rev.*, **130**, 1866 - 1881.

Nicholls, N., C. Landsea and J. Gill, 1998: Recent trends in Australian region tropical cyclone activity. *Meteorol. Atmos. Phys.*, **65**, 197 - 205.

Persing, J., M.T. Montgomery and R.E. Tuleya, 2002: Environmental interactions in the GFDL hurricane model for Hurricane Opal. *Mon. Weea. Rev.*, **130**, 298 - 317.

Pielke, R.A. Jr, C. Landsea, M. Mayfield, J. Laver and R. Pasch, 2005: Hurricanes and global warming. *Bull. Amer. Meteorol. Soc.*, **86**, 1571 - 1575. DOI: 10.1175/BAMS-86-11-1571.

Velden, C., B. harper, F. Wells, J.L. Beven II, R. Zehr, T. Olader, M.Mayfield, C. Guard, M. Lander, R. Edson, L. Avila, A. Burton, M. Turk, A. Ikuchi, A. Christian, P. Caroffe and P. McCrone, 2005: The Dvorak tropical cyclone intensity estimation technique: A satellite-based method that has endured for over 30 years. *Bull Amer. Meteorol. Soc.*, in press.

Walsh, K., 2004: Tropical cyclones and climate change: unresolved issues. *Clim. Res.*, **27**, 77-83.

Webster, P.J., G.J. Holland, J.A. Curry and H.-R. Chang, 2005: Changes in tropical cyclone number, duration and intensity in a warming environment. *Science*, **309**, 1844 - 1846.

Ozone and temperature above Davis, Antarctica, during the austral winter and spring of 2005

A. R. Klekociuk

Ice, Oceans, Atmosphere and Climate Programme, Australian Antarctic Division.

Email: andrew.klekociuk@aad.gov.au

Abstract

A summary of stratospheric measurements above Davis, Antarctica (68.6°S, 78.0°E) for the winter and spring of 2005 is presented. A rapid warming was observed in the lower stratosphere during the third week of August. This was associated with the development of planetary wave activity and warming of the extratropical region between South Africa and Australia. The warming resulted in temperatures being above the frost point for Polar Stratospheric Clouds (PSCs), and produced a change in the character of aerosols above Davis. Despite the warming and its likely influence on PSC volume, total ozone column values above Davis during September were near the minimum values observed by the Total Ozone Mapping Spectrometer (TOMS) for the site. This was likely due to the fact that the warming had taken place after a significant amount of chemical processing of the stratosphere by PSCs had already occurred, and that Davis was still located under the polar vortex.

Introduction

The Antarctic ozone hole of 2005 was amongst the largest on record, being ranked third largest in terms of area as determined from European satellite measurements (WMO, 2006). Winter temperatures in the lower stratosphere over Antarctica were colder than average levels (see Figure 5 of WMO, 2006), but not as cold as during the large ozone hole years of 2000 and 2003. During September and October, minimum daily temperatures poleward of 65°S latitude were near the coldest recorded since 1979 (WMO, 2006).

In this research letter, stratospheric conditions above Davis station during the 2005 winter are summarised using data from ozonesondes, radiosondes and lidar. Davis lies on the Antarctic coast, and based on historical ozone data from satellite instruments such as the Total Ozone Mapping Spectrometer (TOMS) can experience large variations in ozone during late winter and spring. As such, Davis provides a useful site for examining variations in atmospheric dynamics.

Observations

In Figure 1, total column ozone data for Davis are presented from measurements by ozonesondes and TOMS. The ozonesonde measurements during the austral spring of 2005, particularly in September, were generally below the TOMS mean climatology for the years 1997 to 2004, and close to the lowest observed TOMS values. During September, the total column values from the ozonesonde measurements were lower in 2005 than those for the equivalent time in 2004.

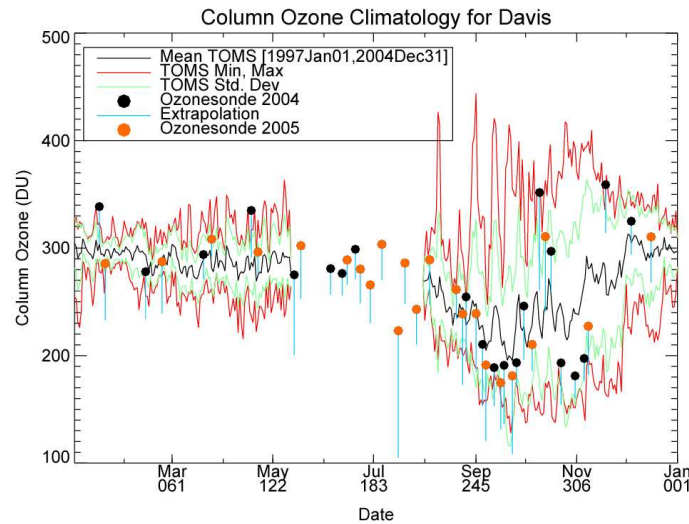


Figure 1 – Total column ozone values from measurements by ozonesondes and the TOMS satellite instrument. The TOMS measurements are normally within 50km of Davis. The vertical blue lines indicate the magnitude of the total ozone column extrapolated above the maximum altitude of the ozonesonde.

The vertical distribution of ozone above Davis is shown in Figure 2. The total column value fell below 220 Dobson Units (the threshold for ozone hole conditions) at the beginning of September. Just prior to this time, during late August, pronounced ozone loss between 12km and 20km was observed.

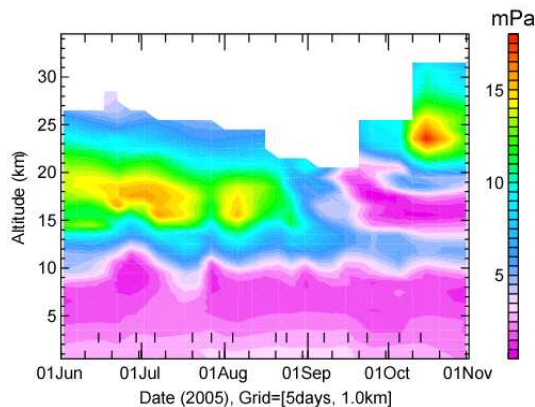


Figure 2. Davis ozone partial pressure from ozonesonde measurements during the winter and spring of 2005. The ozonesonde data have been transformed onto a grid spaced 5 days in time and 1km in altitude. The times of the measurements are shown by the vertical lines above the lower axis. The relatively high partial pressure observed near 23km on October 12 was associated with transport of ozone from low latitudes (see Klekociuk, 2006).

Temperatures in the lower stratosphere and troposphere are shown in Figure 3. As can be seen by comparing Figure 2 and 3, the period of rapid ozone loss in the lower stratosphere was accompanied by a rapid warming of 10-15K. During this time there was a change in the character of stratospheric aerosols, with the disappearance of stratospheric clouds (Figure 4).

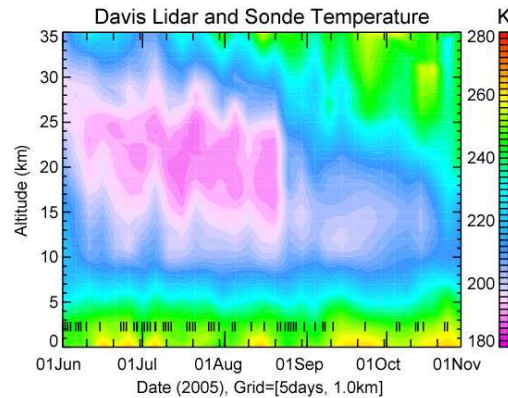


Figure 3. The Davis temperature profile synthesised from lidar and concurrent radiosonde measurements, sampled with the same grid spacing used in Figure 2. The times of the measurements are shown by the vertical lines above the lower axis. Lidar data are used exclusively above 27km altitude.

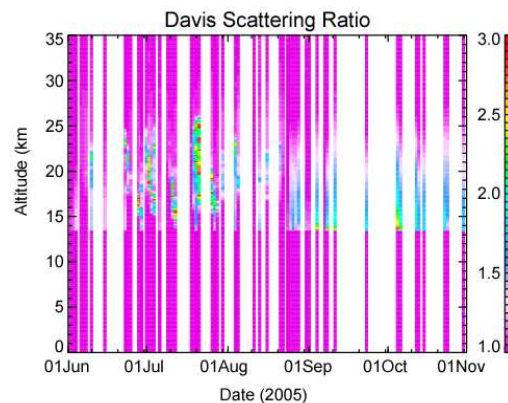


Figure 4. Aerosol loading above Davis as revealed by the lidar scattering ratio (the ratio of the lidar backscatter profile with the backscatter expected from the molecular atmosphere). A scattering ratio above unity indicates the presence of aerosols. Prior to the end of August the aerosol loading was predominantly contributed by layers of Polar Stratospheric Clouds. The change in the character of the vertical aerosol distribution after this time coincides with increased temperatures shown in Figure 3. The lower altitude limit of the lidar measurements was 15km. The molecular density profiles used in the analysis of the lidar data were obtained from the Aura Microwave Limb Sounder satellite instrument.

Discussion

The relationship of Davis to the edge of the polar vortex is shown for the 500K potential temperature surface in Figure 5. For most of the winter and spring period, Davis was well inside the inner vortex edge. In Figure 3, quasi-periodic fluctuation in temperature with a period of approximately 15 days can be seen in the lower stratosphere. These fluctuations were associated with distortion of the vortex by high latitude planetary wave activity. After the third week of August, a belt of warm temperature forced by the planetary wave activity developed northward of Davis (Figure 6) and persisted through the end of October. This feature generally forced the vortex away from Davis and appears associated with the abrupt warming in the lower stratosphere apparent in Figure 3. The temperatures that persisted above Davis from late August were generally above the highest frost point temperature for solid Polar Stratospheric Cloud particles (~195K), and this appears related to the change in character of the aerosols measured by lidar shown in Figure 4.

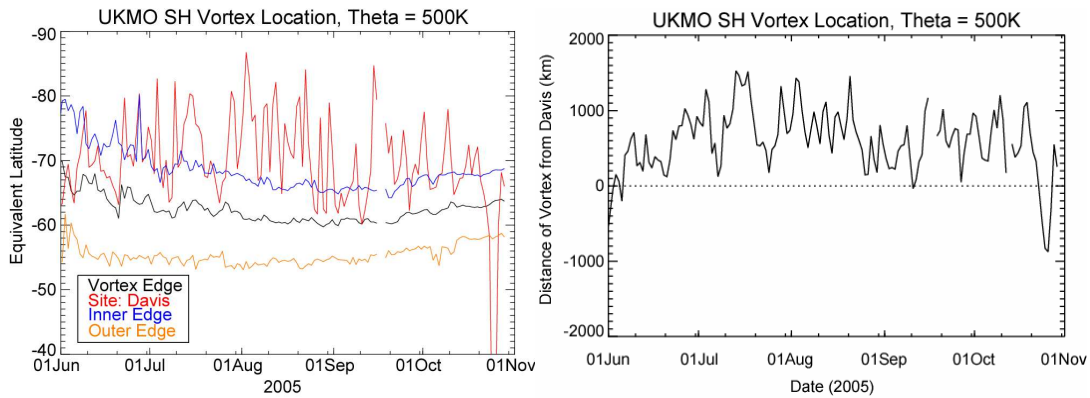


Figure 5. Relationship of Davis to the edge of the polar vortex at the 500K potential temperature surface (approximately 20km altitude). Left; Three definitions of the vortex edge ('inner', 'outer' and central edge) as defined by Nash et al. (1996) are shown in 'equivalent latitude' coordinates, calculated using meteorological fields from United Kingdom Meteorological Office (UKMO) Stratospheric Assimilated Data. The red curve shows the equivalent latitude of Davis; where this is more poleward than that of the vortex edge, Davis is regarded as being inside the vortex. Right; Distance of Davis from the 'central' vortex edge (positive values mean that Davis is inside the vortex).

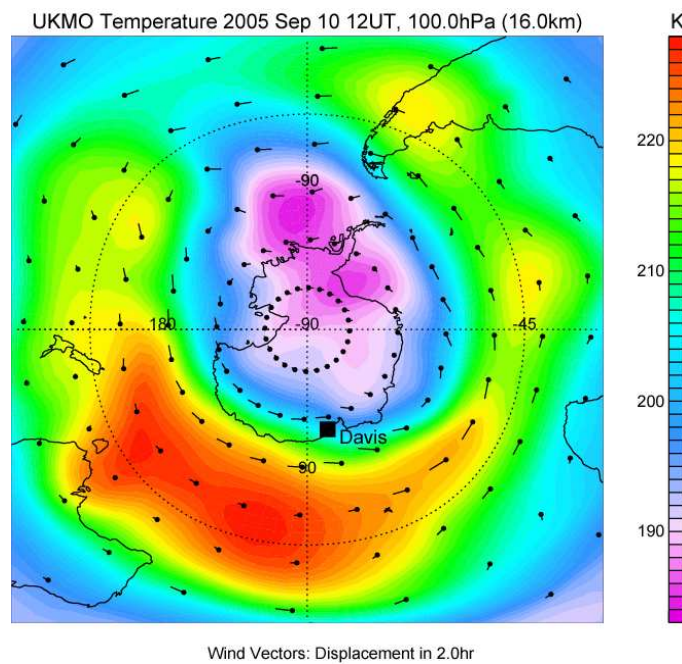


Figure 6. Temperature map for 10 September 2005 at the 100hPa pressure level from UKMO Stratospheric Assimilated Data. A belt of warm temperatures was situated northward of Davis. This warm temperature region persisted in the sector between South Africa and Australia during most of September and October.

Conclusions

Low ozone concentrations associated with the ozone hole were observed in the lower stratosphere above Davis, Antarctica during 2005. An abrupt warming was observed in the lower stratosphere above the site during the third week of August in 2005. This was due to planetary wave activity in the extra-tropical region, and movement of the

polar vortex edge towards Davis. Despite the warming and its likely influence on reducing chemical processing of the atmosphere by PSCs, Davis was still located within the vortex, and observed low ozone levels associated with the ozone hole.

Acknowledgements

This paper was prepared under Australian Antarctic Science Project 737. Thanks are due to Andrew Cunningham (Australian Antarctic Division) for collecting the lidar data, to Mark Austin and Kevin Gunn (Australian Bureau of Meteorology; BoM) for launching the ozonesondes, and to Jim Easson (BoM) for processing the ozone data. Radiosonde data were supplied by BoM. United Kingdom Meteorological Office Stratospheric Assimilated Data were obtained through the British Atmospheric Data Centre (<http://badc.nerc.ac.uk>) and data from the Aura Microwave Limb Sounder were obtained from the NASA Goddard Spaceflight Center (<http://disc.gsfc.nasa.gov/Aura/MLS>).

References

- Klekociuk, A.R. Meridional transport of low-latitude stratospheric air to the Antarctic region, BMRC Research Letters 4, 2006 (this issue).
- Nash, E.R., P.A. Newman, J.E. Rosenfield, M.E. Schoeberl An objective determination of the polar vortex using Ertel's potential vorticity. *J.Geophys.Res.*, 101, 9471-9478, 1996.
- WMO (World Meteorological Organisation), Antarctic ozone bulletin winter/spring summary, 8/2005, 2006 (<http://www.wmo.ch/web/arep/05/bulletin-8-2005.pdf>)

An Examination of Dewpoint Biases Introduced by Different Instrumentation

Chris Lucas

Bureau of Meteorology Research Centre, Australia

Email: c.lukas@bom.gov.au

Introduction

Correct measurement of atmospheric water vapour is crucial for understanding the observed circulation on all time scales. New technologies for measuring humidity have come into use due to the widespread deployment of Automatic Weather Stations (AWSs) in Australia since the 1990s. As with all instrumentation, different techniques and methods result in different answers. The aim of this paper is to understand the causes and effects of the dewpoint measurement differences produced by the various instruments used by the Bureau of Meteorology (BoM).

This paper is an outgrowth of a project to produce a high-quality, homogenous humidity database across Australia. A necessary step in the homogenization procedure is correcting the effects of changes in instrumentation. As the project progressed and the differences in dewpoint due to instrumentation effects became apparent, the need for a shorter contribution dedicated explicitly to this subject became obvious.

The approach for this study is a statistical examination of data from a wide range of stations. The responses of the instrumentation are examined on a seasonal to annual time scale and are based on the results of the homogenization procedure. In this document, a basic overview of the homogenization procedure is given. A complete description of the procedure is the subject of a BMRC Research Report currently under preparation. The methodology and instrumentation of atmospheric humidity measurement used by the BoM is reviewed. Dewpoint biases are estimated and analysed, based on the different instrument types. The sources of biases and the effects of climate variability are then examined. The main findings are summarized in the conclusions.

Creation of a Homogeneous Dewpoint Dataset

The goal of data homogenization is to remove the effects of station discontinuities -- for example, those caused by changes in station location and/or observation procedures -- from a time series of a variable (dewpoint in this case) at a given *candidate station*. Fifty-four candidate stations are used in this study. Coverage extends across Australia. In general, these stations are high-quality sites located at airports and meteorological offices. Some lower-quality stations, such as those at post offices, are included for spatial completeness. As a rule, these stations have nearly continuous observations extending from 1957 through 2003. Records at five stations start slightly later than this.

To homogenize the record at a candidate station, it must be compared to a *reference series* free from inhomogeneities. Since few, if any such stations exist in the records, a composite reference series must be created from *reference stations*. These are nearby stations with records of reasonable quality and length (pre-1980 is the minimum length criterion chosen here) and a humidity climate similar to the candidate station. Some leeway exists in the definition of ‘nearby’; many remote Australian stations simply do not have any suitable stations within 200-300 km, forcing the selection of less-than-ideal reference stations. At a given candidate station, between 4 and 9 reference stations are chosen to create the reference series.

At the candidate and reference stations, time series of morning (0800 or 0900 local time) monthly median dewpoint are seasonally averaged (e.g. DJF, MAM...). The long-term seasonal means are removed from these series to create seasonal anomalies. These are the basic time series used in this analysis. To create the composite reference series, the technique described by Peterson and Easterling (1994) is generally followed. In this method, a consensus *difference series*, the difference of a given point from the previous one in the series, is derived from a correlation- and distance-weighted average of the difference series at the reference stations. Difference series minimize the effects of a discontinuity in a long record. The consensus series is then integrated backward in time to create a composite homogeneous reference series. The reference series is subtracted from the candidate series. This time series is subsequently used to identify inhomogeneities in the data.

Humidity Measurement Methodology and Instrumentation in the BoM Psychrometric Method

In Australia, the psychrometric method is most often used to measure humidity in the atmosphere. In this method, the actual amount of vapour in the air is determined from two simultaneous, but separate temperature measurements:

- 1.) the ambient air (‘dry-bulb’) temperature and 2.) the wet-bulb temperature.

The wet bulb temperature is measured by wrapping the bulb of the thermometer in a wick, which is kept wet with distilled water. This allows a measurement of the amount of cooling produced by evaporation, a quantity dependent on the relative humidity (RH). A value for station pressure is also required.

The various measurements are subsequently used in the semi-empirical psychrometric formula

$$e_s(T_d) = e_s(T_w) - Ap(T - T_w),$$

where $e_s(T_d)$ is the saturation vapour pressure at the dewpoint, $e_s(T_w)$ is the saturation vapour pressure at the wet-bulb temperature T_w , p is the pressure, T is the ambient air temperature and A is the psychrometric constant. Saturation vapour pressures are converted to and from their associated temperatures using the approximation derived by Alduchov and Eskridge (1996) with the small ‘enhancement factor’ based on pressure omitted:

$$e_s(T) = 6.1094 \exp\left(\frac{17.625T}{T + 243.04}\right).$$

The psychrometric constant A defined above is a critical term and a major source of uncertainty in the calculation. From a purely thermodynamic standpoint, $A = c_p (\epsilon L)^{-1} \approx 6.46 \times 10^{-4} \text{ K}^{-1}$ at 0°C . However, the value of this ‘constant’ when making real-world measurements varies considerably based on a number of factors.

The most important of these factors is the ventilation of the instrument and/or its shelter. Figure 1 shows schematically the response of A to changes in the ventilation. At low ventilation speeds, A is high. As ventilation speeds increase above $\sim 3 \text{ m s}^{-1}$, A decreases asymptotically. Another important factor in determining A is the design of the wet bulb sensor.

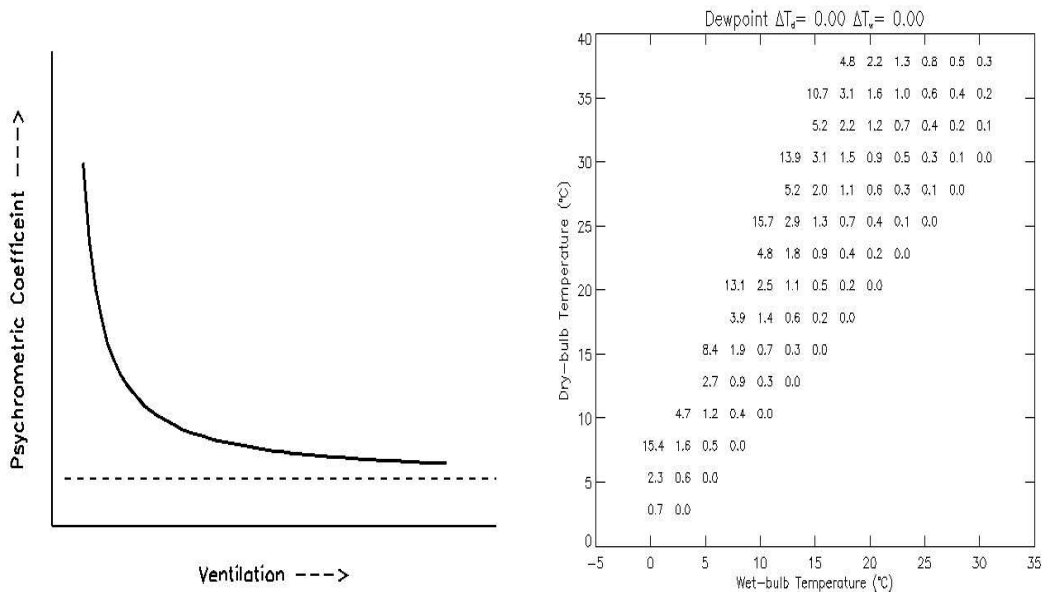


Figure 1 (left) Schematic diagram of variation of psychrometric coefficient A with changes in the ventilation of the instrument. And Figure 2 (right) difference in dewpoint at selected dry- and wet-bulb temperatures due to a change in the value of the psychrometric coefficient. This plot is the difference with $A = 7.00 \times 10^{-4} \text{ K}^{-1}$ from $A = 7.886 \times 10^{-4} \text{ K}^{-1}$.

Psychrometric measurements made by the Bureau of Meteorology use ‘naturally ventilated’ screens, with values of A recommended by the Commission for Instruments and Methods of Observations Guide (CIMO, 1996) to be $7.7\text{-}8.0 \times 10^{-4} \text{ K}^{-1}$ for wet-bulb temperatures in excess of 0°C . The standard Bureau value of $7.886 \times 10^{-4} \text{ K}^{-1}$ falls within this range, and is used in all calculations in this study.

Figure 2 shows the sensitivity of the computed dewpoint to a change in the value of A . In the figure, the value of A is set to $7.000 \times 10^{-4} \text{ K}^{-1}$. (The reason for choosing this value will become apparent later). Dewpoints computed using this value of A are subtracted from those with the standard value. The lower value of A results in a higher dewpoint being measured. If the value of A used in Figure 2 were the true value and the standard is instead used, then these numbers in the figure are the negative bias that results. This effect is more pronounced at lower RH, where the dewpoint errors can be quite large. The magnitude of this error reflects the non-linear relation between vapour pressure and dewpoint. Even at higher RH, the dewpoint errors are potentially on the order of 0.2 degrees or so.

Instrumentation

Historically, the primary instruments used to measure humidity have been mercury-in-glass (Hg) thermometers. These are standard instruments that derive temperature by measuring the rise and fall of a column of mercury as it expands and contracts with changes in temperature. These instruments were used over most of the country until the gradual introduction of AWSs, beginning in earnest in the early-1990s. They are still in use in many AWSs, as supplemental readings. Five candidate stations in the dataset exclusively used Hg thermometers in 2003 and Typically 50-75% of the reference stations employed Hg thermometers, although this number varies from around 15% to 100%.

Most AWSs in the humidity database use values derived from platinum resistance thermometers (PRTs), which work by measuring the temperature-dependent change in the resistance of a conductor, in this case platinum. The instruments used in Australia are manufactured by Rosemount, and are referred to as 'temperature probes'. AWSs using PRTs rely on the psychrometric method to measure humidity, with a dry- and wet-bulb probe. Of the 54 stations in the dataset, 39 used PRTs in 2003. At more remote stations, military bases and other stations where staff are not on hand to maintain the instruments (particularly the wet-bulb thermometer), electrical humidity measurements are made using a humidity probe (HP). This instrument does not require the techniques of psychrometry, but instead measures the humidity directly by measuring the change in capacitance of a thin film, a quantity dependent on the RH. These devices typically have a larger uncertainty in their measurement and are generally not reliable in the long term as they are subject to hysteresis and drift after exposure to very high RH and cloud (e.g. Strangeways 2001). Through 2003, ten of the stations in the dataset used HPs and the majority of AWSs with HPs installed used devices manufactured by Rotronics of Switzerland.

The sitesDB – metadata database - also indicates that other instruments have been used to measure humidity at different times and different stations. Before the 1990s, many stations used hygrographs or thermohygrographs to record humidity as well. Other stations show the use of psychrometers and hair hygrometers in their records. In general, these instruments were not the 'official' measurement, but rather a supplemental one to the Hg thermometer standard.

Estimates of Dewpoint Bias in 2003

The dewpoint bias at a given candidate station is estimated by averaging the difference between the candidate and reference series seasonal anomaly over the last 4 seasons (DJF03, MAM03, JJA03 and SON03). Figure 3 shows a scatterplot of the calculated bias against the linear trend of the candidate series. Examining the distribution of points along the ordinate reveals a distinct skew towards negative biases in the estimates.

There are several possible sources of the observed bias. Potential sources of bias include errors in calibration, an artificial bias introduced by an incorrect seasonal mean dewpoint resulting from a long-term linear trend in the data or biases introduced by the different instruments used. Some combination of these effects is also possible.

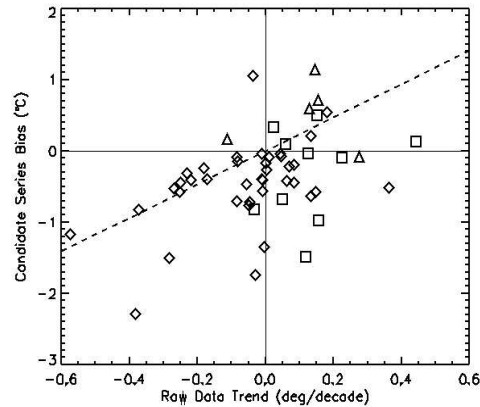


Figure 3. Raw data trend against the calculated the observed bias in the candidate series for all 54 stations. Symbols refer to instrument type, where diamonds are PRTs, squares are HPs and triangles are Hg thermometers. The dashed line is the bias expected due to a linear trend.

The instruments and their calibrations are typically checked once or twice a year. If the instrument exceeds its tolerance, it is repaired or replaced. The values of the offsets (for the electrical instruments) are recorded and stored in the sitesDB. Using the calibration information for the dry and wet bulb combination (PRTs) or errors in RH (HPs), an estimate of the dewpoint bias can be obtained. The HP calibration numbers are erratic in many cases, and are not particularly reliable. For the PRTs, the calibration offsets show a slight skew towards negative values. Most values are less than 0.3 degrees in magnitude, with a mean of -0.14 degrees. There is essentially no correlation between the observed PRT bias and the calibration offset (Table 1 last line).

variable	R	coefficients
constant	--	-0.170
Hg	-.433	-.450
DP	.344	1.72e-2
dist	-.251	-7.50e-4
trend	.262	--
cal	-.045	--

Table 1. PRT station correlations of potential regression variables with observed bias and regression coefficients for the variables selected for the outlier removed cases. See text for description of variables

Another possible explanation is a bias created by the long-term linear trend seen in the candidate series. Assuming the dewpoint is reasonably accurate at the end of 2003, a long-term negative trend will result in an overestimate of the seasonal mean dewpoints. When anomalies are computed, the incorrect seasonal mean will result in a negatively biased seasonal anomaly. In cases where a positive trend is observed, oppositely signed seasonal means and anomalies will be seen. For the 47 years of the typical series, the effect should account for 0.235 degrees of dewpoint bias for every 0.1 degrees/decade of trend.

Returning to Figure. 3, there is an apparent strong relationship between trend and bias ($r = +0.44$). However, the points with trends < -0.15 deg/decade are producing much of this correlation, and removing even some of these points greatly reduces the correlation. The predicted bias due to the trend is plotted as the dotted line. The

majority of the points are well off this line. Still, there are several stations near the predicted 'trend bias' line and several of these fall within $\pm 25\%$ of the predicted value, suggesting that this effect is responsible for some of the observed bias. With the exception of these cases, generally where a strong negative trend is observed, the trend in the raw data apparently has only a minor role in producing the observed bias in the last year of the record.

More significantly, Figure 3 shows that the type of instrument used in the last years of the record appears to have an effect on both the trend and the bias of the candidate series. At stations equipped with PRTs, the stations tend to have negative biases and low and more negative trends. Candidate stations with Hg thermometers generally have both a positive bias and trend. Stations using HPs are mixed in their biases, but generally have positive trends. There are exceptions to this general behaviour for each instrument. In the next sections, possible explanations these observations of PRTs and HPs will be examined.

Sources of Instrumental Bias in Platinum Resistance Thermometers

Thirty-six of the 39 candidate stations with PRT wet-bulb sensors show negative biases. A mathematical model of the average bias at stations using PRTs is constructed using multiple linear regression (e.g. Draper and Smith, 1981). The goal of this model is twofold. The first is to identify the important sources of the observed bias. The second is to estimate a typical offset of PRTs from Hg thermometers. Five variables in different combinations are tested.

These variables are:

1) the fraction of reference stations with Hg thermometers (*Hg*); 2.) the annual average dewpoint (*DP*); 3.) the distance between the candidate and its nearest reference (*dist*); 4.) the linear trend in the raw data (*trend*); and 5.) the calibration offset based on the numbers in the sitesDB (*cal*).

The regression equation that explains the most variance with the lowest standard error is kept.

With all stations included, the trend is by far the dominant variable regardless of which combination is used. However, as noted in the previous section, the trend alone does not do a particularly good job at explaining the observed biases. Most points lie well off the predicted line. Including other variables does not result in a great improvement to the fit. The most significant regressions involve *Hg* and *trend*. Examining the residuals (not shown) for these fits reveals the existence of several outlier points.

These same outliers are also apparent in Figure 3. Seven stations with strong positive ($>0.5^{\circ}\text{C}$) or negative ($<-1.0^{\circ}\text{C}$) biases are removed and the regression is rerun. Three of the deleted stations (Cape Leeuwin, Brisbane AP and Alice Springs) have artefacts in the data or analysis. The remaining four stations (Longreach, Meekatharra, Rabbit Flat and Kalgoorlie) have very strong negative biases. The source of these exceptional biases is explored further in a later section.

Table 1 summarizes the results of the regression analysis. Removing the outliers creates significant correlations of observed bias with *Hg* and *DP*. The correlation with *trend* is much reduced, and is now insignificant. The correlations with *cal* and *dist* are about the same. For the regression, the best fit is obtained with variables *Hg*, *DP* and *dist*. With these variables, about 36% of the variance is explained. The residual plots (not shown) do not suggest any outliers. Including *trend* reduces the significance of the fit and slightly increases the standard error.

For a PRT-equipped station with an annual average dewpoint of 10°C, the regression equation predicts an offset of -0.4 to -0.5 degrees from a collocated Hg thermometer. The standard error of 0.2 for the regression is large, about 50% of the mean. However, the BoM technical documents discussed in subsequent paragraphs suggest that the model is at least capturing the gross effects responsible for the bias.

In a comparison of the response of Hg thermometers and PRTs across a variety of conditions, Warne (1998) found that Hg thermometers overestimate the dewpoint relative to PRTs. While both instrument types had errors, which increased with decreasing RH, the Hg thermometers generally had higher dewpoints.

Gorman (2003) compared dewpoints at an operational AWS using PRTs with a calibrated reference standard. In that study, the AWSs produced lower dewpoints, especially at lower ambient RH values. The wind speed was a crucial factor, suggesting this was a result of better ventilation of the screen, and a correspondingly lower value of *A*. Lowering *A* to $7.00 \times 10^{-4} \text{ K}^{-1}$ gave a better fit to the reference data. Physically, it was suggested that this was due to the ventilation characteristics of the small Stevenson screen being poorly characterized. However, a tabulation of the screen types at the candidate and reference stations reveals that the vast majority of screens in Australia during 2003 are of the 'small' type. Using this fact and the findings of Warne (1998), it is hypothesized that the difference in *A* are due to the ventilation characteristics of the PRT rather than the screen.

These findings are consistent with the biases observed at PRT-equipped candidate stations. Mercury thermometers are the primary wet-bulb instrument at many reference stations. Further, PRT-derived dewpoints are artificially low due to an incorrect value of *A*. These factors combine to produce a negative bias, which is more negative where *Hg* is larger and the humidity (*DP*) is lower. This reasoning is in general agreement with the regression model. The *dist* influences the bias indirectly. A highly significant negative correlation (~-0.5) is observed between the average annual RH and *dist*. Stations with greater spacing tend to be in the more remote, drier regions of the continent. As previously noted, lower humidity results in a higher bias. Including *dist* explains more variance and has a lower standard error than directly including the RH or leaving the variable out of the regression.

Humidity Probes

At the HP stations, the observed bias response varies quite a bit. Four of the 10 stations have biases with a magnitude of less than 0.2 degrees (Figure 3). Two have higher positive biases; four have strong negative biases. To investigate factors that

influence the bias, a regression analysis is performed, using similar variables. Calibration data is very inconsistent at a given station for the HPs and hence not included. The annual average rainfall (*rain*) is included to reflect the propensity of the instrument to experience extremely high RH conditions, which can adversely affect its operation.

The results of the analysis are shown in Table 2. With so few stations, only the correlation with *DP* is significant. Reasonably high (but insignificant) correlations are also seen with *Hg* and *rain*. In the regression, it is found that the fit using *DP* and *rain* has the lowest standard error. Including *Hg* also provides a good fit, although it is not as significant as without. For Australian-average rainfall (472 mm) and a mean dewpoint of 10°C, a typical bias value of -0.3 degrees is estimated from the equation. However, the standard error is 0.37 and considerable variation should be expected as the variables used in the regression suggest that the main factor determining the bias is the climate where the instrument is placed. In drier climates with little rain, positive biases are indicated.

variable	correlation	coefficients
constant	--	1.315
<i>Hg</i>	-.363	--
<i>DP</i>	-.752	-0.137
<i>dist</i>	.107	--
<i>trend</i>	.242	--
<i>rain</i>	-.369	-5.683e-4

Table 2. HP station correlations of potential regression variables with observed bias and regression coefficients for the selected variables.

These results are consistent with the findings of BoM internal test reports on this HP. Huysing (1995) showed that the biases of the Rotronics probes varied with the ambient RH at the station, with positive biases at low RH and negative biases at high RH. This matches the direction of the regression with variable *DP*. Gorman (2001) suggests systematic errors in the probes due to 'inaccuracies in the potentiometer adjustment' are on the order of 2%. This offset is not constant, but inconsistently varies with the RH. This is on top of a random error of 1%. These findings translate to an uncertainty in dewpoint on the order of 0.9°C.

Analysis of the residuals indicates three sites that have unusual behaviour. These stations are Bourke, Laverton and Camooweal. At Camooweal, the Rotronics probe was not used after 2002. Rather, a Vaisala humidity probe is used, which is shown by Gorman (2002) to have different response characteristics than the Rotronics HPs. The large residuals at Bourke and Laverton likely reflect the shortcoming of using an annual measure of humidity. While *DP* is nearly identical at the stations, the annual cycle of dewpoint at the stations is quite different. The large differences in the observed bias to nearly identical values of the predictor create 'pure error' in the regression. Another possible explanation for this behaviour could be calibration differences in the probes.

Climate, the Psychrometric Coefficient and Bias

A 'typical bias' value of -0.4 to -0.5 for PRT-based humidity measurements is predicted by the regression equation. This value is broadly consistent with the suggestion of Gorman (2003) that a lower value of A is required for AWSs using PRTs (Figure 2). This number is most suitable for use on seasonal to annual time scales. On, say, a daily time scale the bias may be much different depending on the weather. For normal meteorological variability, the biases typically 'average out' to produce something like the typical bias. However, if drier conditions persist due to longer-term climate influences the observed bias may vary considerably from the predicted value. Further, such climate anomalies are often regional in scope, rather than continent wide. These vagaries of climate response are likely partially responsible for the high standard error of the regression equation.

In much of Australia, conditions were generally hot and dry during 2002 and 2003. This was especially noteworthy in interior NSW and QLD (BoM, 2003; 2004), and was related, at least in 2002, to the warm phase of the El Niño-Southern Oscillation. Mean annual temperature anomalies were on the order of 0.5 to 1.5 degrees above the long-term mean in both years. Annual rainfall deciles ranged from 1-4, very much below average to average, with some portions of the region reporting the 'lowest ever' seasonal rainfall values. The higher temperatures and lack of rain produce generally lower values of RH.

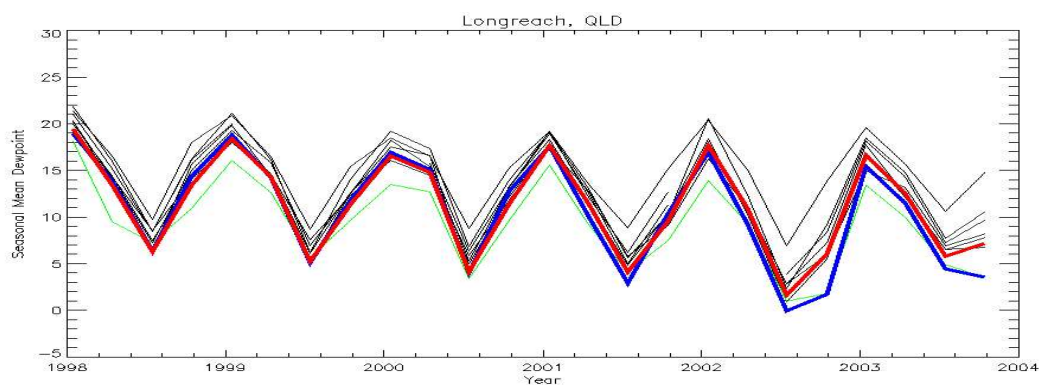


Figure 4. Longreach, QLD. time series of seasonal mean dewpoint from 1998 to 2003. Shown are the raw candidate series (thick blue line), the computed reference series (thick red line) and the eight reference station series (thin line) used in computing the bias. The Charleville reference station is shown as the thin green line. An additional offset of 3.6 degrees has been applied to the reference series.

This effect of these climate anomalies is illustrated in Figure 4, the seasonally averaged dewpoint time series of the candidate and reference station data from Longreach, QLD. A general downward trend in seasonal mean dewpoint is seen during this period at all stations and in the reference series. However, in JJA02, SON02 and SON03 in particular, the candidate station is well below both the reference series and the vast majority of reference stations. Calibration data collected from sitesDB suggest a calibration error in dewpoint on the order of -0.6 degrees at this station throughout 2002-3, but this is not large enough to account for the dewpoint anomalies seen here.

Similar variations were widespread during this time period among PRT stations, particularly in QLD and northern NSW. One such station is Charleville, QLD, also shown in Figure 4. The dewpoints at Charleville mimic those at Longreach, further suggesting this is a climate impact on the value of A . Stations in the interior of WA also show this effect. The magnitude of the effect seems to vary. This may be due to differences in the climate response or other regional variations. Other factors, such as uncertainties in the calibration or other maintenance issues could also play a role.

Conclusions

Biases in humidity measurements are examined from a statistical standpoint. Carefully constructed humidity reference series from 54 stations across Australia are used to estimate biases during 2003. The majority of the humidity observations from stations that make up the composite reference series are made with traditional mercury-in-glass thermometers. The candidate stations use either Hg thermometers, platinum resistance thermometers or humidity probes. The bias is computed relative to this reference series. Potential causes of the bias include calibration errors, biases due to long-term trends and instrumental effects. The results suggest that instrumental biases are the most important.

Stations that rely on platinum resistance thermometers for their measurements generally have a dewpoint bias with a nominal value of -0.5 degrees. Stations that use humidity probes have a dewpoint bias with a nominal value of -0.3 degrees. As noted before, the bias is computed relative to the reference series; hence, it cannot be stated unequivocally which measurement is the correct one.

The results here indicate that the climate at the site of the dewpoint sensor plays a crucial role in the subsequent performance of the instrument. For the HPs, the amount of bias predicted by the regression depends solely on climate variables, namely the average annual dewpoint and the average annual rainfall. However, particular care should be taken in interpreting this result, due to the small sample size and the inherent uncertainty in HP design. The bias characteristics at HP stations are also likely to change as the Rotronics probes are phased out and replaced with Vaisala probes.

For the PRTs, the situation in regards to climate is more complex. The average annual dewpoint is one of three variables that influence the bias in the regression. The other two have to do with construction of the reference series. Physically, the amount of observed bias is consistent with an incorrect value of the psychrometric coefficient A associated with the PRT. The climate *variability* is also a factor, although not accounted for in the regression. During extended hot and dry periods, such as those associated with El Nino, the effect of the mischaracterization of A can be magnified, resulting in even larger biases. Such an effect was observed in 2002 and 2003.

The results of this study, together with the results of the referenced instrument test reports, provide a solid basis for further study of this problem. The amount of bias has been quantified and some mechanisms for the sources proposed. The uncertainty in the value of A needs to be addressed. Ideally, further experiments and instrument tests

in both the laboratory and the field would be performed. The climate of the location where the instrument is sited should be accounted for in any such study.

References

Alduchov, O. A. and R. E. Eskridge, 1996: Improved Magnus form approximation of saturation vapor pressure. *J. Appl. Meteor.*, **35**, 601-609.

BoM, 2003: *Annual Australian Climate Summary 2002*. Available from http://www2.bom.gov.au/announcements/media_releases/climate/change/20030106.shtml

BoM, 2004: *Annual Australian Climate Summary 2003*. Available from http://www2.bom.gov.au/announcements/media_releases/climate/change/20040105.shtml

CIMO, 1996: Guide to Meteorological Instruments and Methods of observations, WMO No 8, World Meteorological Organisation, Ch 4.

Draper, N. R. and H. Smith, 1981: *Applied Regression Analysis*, 2nd Ed. John Wiley and Sons. 709 pp.

Gorman, J., 2001: Evaluation of the output variability of Rotronics MP101A humidity probes. BoM Instrument Test Report number 659, 13 pp.

Gorman, J., 2002: Evaluation of Vaisala HMP45D humidity probes. BoM Instrument Test Report number 661, 20 pp.

Gorman, J., 2003: AWS determination of dew point in the field. BoM Tech. Note 2003-0001_revision1, 27 pp

Huysing, P., 1995: Performance tests on a Rotronic MP101A humidity/temperature probe. BoM Instrument Test Report number 641, 5 pp.

Peterson, T. C. and Easterling, D. R., 1994: Creation of homogeneous composite climatological reference series. *Int. J. Climatol.*, **14**, 671-679.

Strangeways, I., 2003: *Measuring the Natural Environment, 2nd Edition.*, Cambridge University Press, 534 pp.

Warne, J., 1998: The practical impacts of RTD and thermometer design on wet and dry bulb relative humidity measurements. BoM Instrument Test Report number 648, 6 pp.

Meridional transport of low-latitude stratospheric air to the Antarctic region

A. R. Klekociuk

Ice, Oceans, Atmosphere and Climate Programme, Australian Antarctic Division.

Email: andrew.klekociuk@aad.gov.au

Abstract

An episode of anomalous enhanced ozone concentration in the mid-stratosphere above Davis, Antarctica (68.6S, 78.0E) during October 2005 has been linked to a filament of tropical ozone-rich air that was forced to high latitudes by a disturbance to the circulation of the polar vortex. From consideration of lidar and satellite measurements, it is concluded that the air in the filament was also associated with layered and enhanced aerosol concentration. Temperature and wind shears associated with the filament are likely to have been dynamically driven, and may have been a source of small-scale wave activity as well as promoting the sorting and enhancement of aerosols.

Introduction

On 12 October 2005, ozone concentrations in the mid-stratosphere as measured by an ozonesonde launched from Davis station in Antarctica appeared unusually high in comparison with normally observed levels. In WMO (2005), evidence linking this event to transport of low-latitude air to the Antarctic region was discussed. In this research letter, further analysis of the event is presented.

Observations

Regular measurement of the vertical ozone profile above Davis has been conducted since February 2003 using ECC ozonesondes. The ozonesonde flights have been made weekly between mid-May and mid-October, and monthly from November to April. A Rayleigh lidar at the site (Klekociuk et al., 2003) is used to measure the vertical temperature and aerosol profile during the ozonesonde flights.

The Davis ozone profile for 12 October 2005 is compared with other ozonesonde flights in figure 1. The ozone mixing ratio exhibited a 'knee' region near 23km altitude, and a peak at 30km.

Temperature data for the vicinity of Davis showed an inversion in the mid-stratosphere, with a peak near 25km, and a minimum near 35km (figure 2).

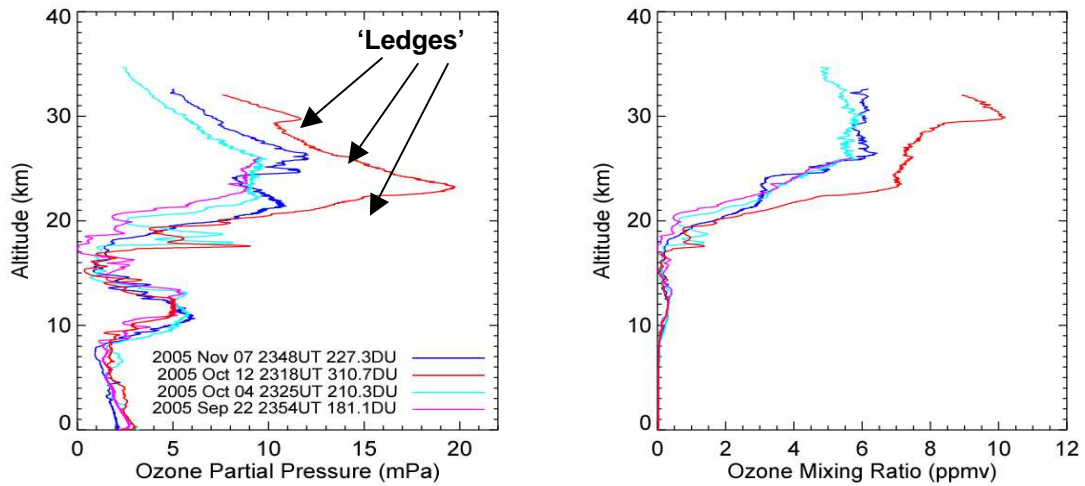


Fig. 1 – Comparison of ozone partial pressure (left) and ozone mixing ratio (right) profiles obtained at Davis between September and November 2005. The region between ~12km and ~20km altitude shows reduced ozone levels associated with the ozone hole. The measurements on 12 October (red curve) are noticeably higher above 20km altitude than the other observations. The legend indicates the inferred total column amount (in Dobson Units; DU) for each observation. Arrowed features in the left hand plot are discussed in the text.

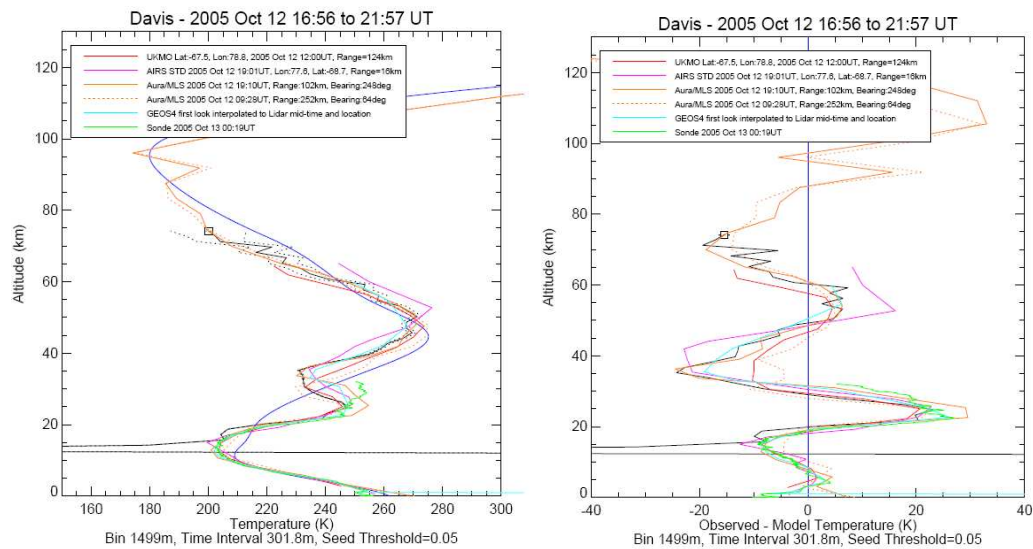


Fig. 2 – Comparison of Davis lidar temperature profiles with other data sources, including the United Kingdom Meteorological Office (UKMO) Stratospheric Assimilated Data, the Atmospheric Infrared Sounder (AIRS) suite of instruments on the Aqua satellite, the Microwave Limb Sounder (MLS) on the Aqua satellite, the NASA/Goddard Global Earth Observing System version 4 atmospheric assimilation (GEOS4), the Mass Spectrometer Incoherent Scatter Extended version 2000 (MSISE-00) atmospheric assimilation, and radiosondes. The lidar measurements have been seeded using an Aura/MLS temperature measurement at the altitude where the one standard deviation relative density uncertainty was 5% (marked by a box near 75km altitude). The lidar observations below 27km altitude have been for the attenuation effects of a mechanical shutter. Correction has also been applied for molecular attenuation (using atmospheric densities inferred from the Aura/MLS temperature profile and a function of altitude) and ozone attenuation (using data from the ozonesonde observation). Right; Differences of the temperature profiles from MSISE-00 for the relevant time and geographic location.

Comparison of the profiles in figure 2 suggests that there were significant temperature changes near the altitude of the inversion. For example, Aura/MLS profiles separated by less than 10 hours differed by approximately 20K at 35km. High resolution temperature measurements are presented in figure 3.

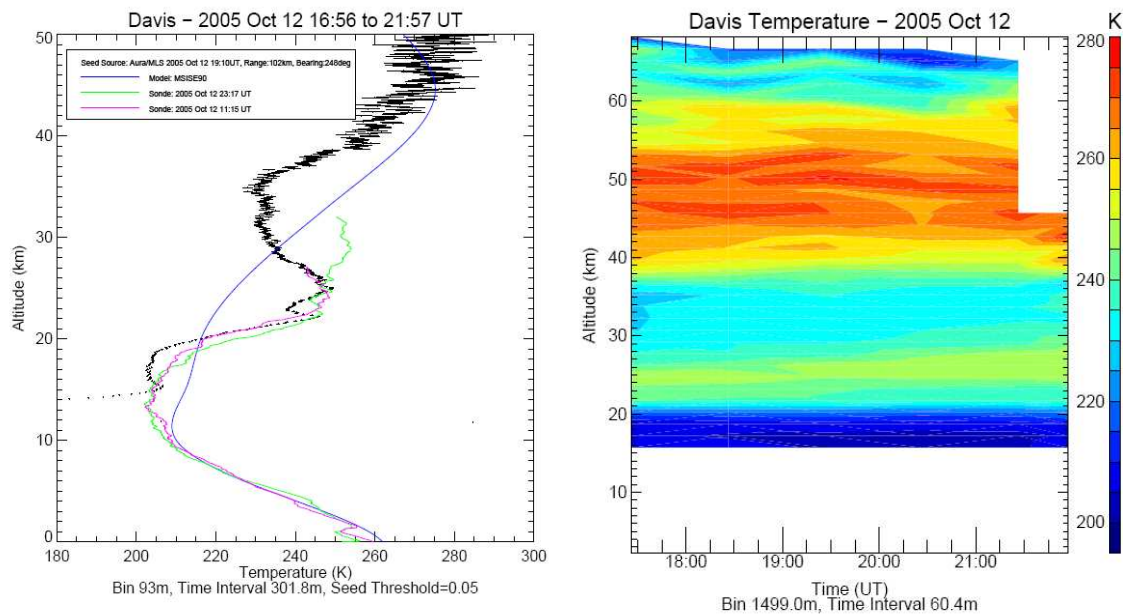


Fig. 3 – (Left) Comparison of high vertical resolution lidar and radiosonde temperature profiles. The lidar data are shown with an error bar spanning one standard deviation. (Right) Altitude-time contour display of 1.5km vertical resolution hourly lidar temperature profiles. The lower altitude limit of the lidar temperature retrieval is 15km.

The lidar temperature retrieval assumes that the atmosphere consists of a perfect gas in hydrostatic equilibrium, and has a cold bias where aerosols contribute to the backscatter. During the spring at Davis, the stratospheric aerosol layer normally has a maximum altitude of about 35km. The presence of aerosols is inferred from the lidar scattering ratio, which is the ratio of the lidar-derived density to the density of the purely molecular atmosphere.

In figure 4, lidar scattering ratio data are shown for October 12 using concurrent Aura/MLS measurements to infer the molecular density profile. The scattering ratio profile shows a pronounced layer near 23km, and broader layers near 29km and 18km. The broader layers are also apparent during the previous and subsequent observing sessions. There is also the indication from the right hand panel of figure 4 of slow temporal changes to the layers, particularly above 25km altitude. As shown in figure 5, the narrow layer at 23km appears to coincide with the altitude of maximum wind speed.

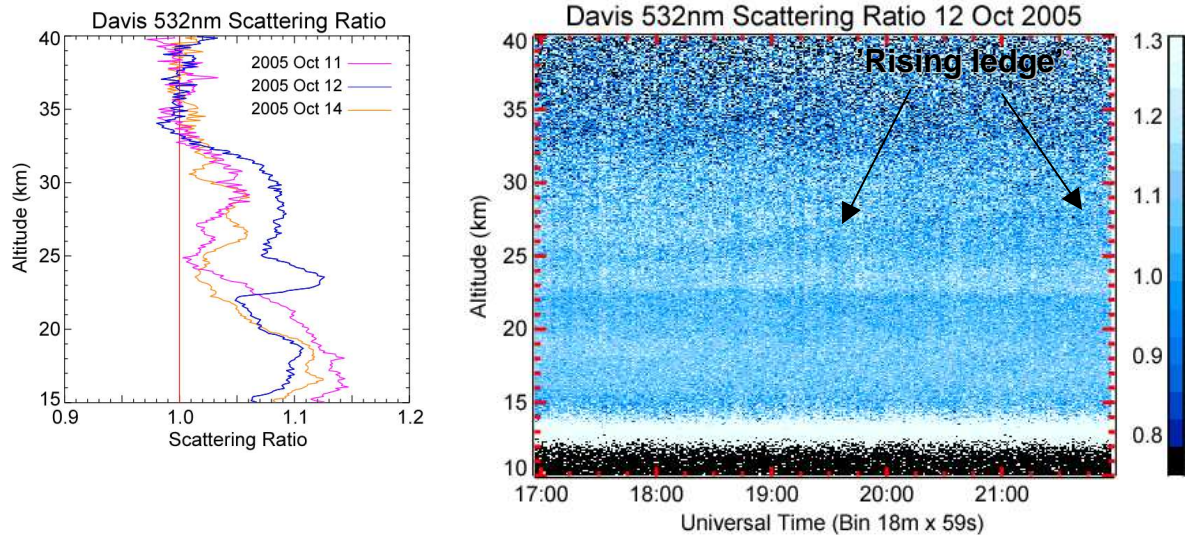


Fig. 4 – Profiles of lidar scattering ratio (the ratio of the observed lidar signal to the expected signal for a purely molecular atmosphere) at a wavelength of 532nm. Left; Comparison of scattering ratio profiles for October 11, 12 and 14. In each case, the molecular density profile has been derived from the closest (in time and distance) Aura/MLS profiles of temperature and pressure (interpolated to the lidar measurement bins from Aura/MLS geopotential heights converted to approximate geometric heights). The scattering ratio is normalised to unity over the altitude range [35,40]km. A correction for ozone attenuation on 12 October has been made using the concurrent ozonesonde measurement, while the profiles for 11 and 14 October have been corrected using the UARS Reference Atmosphere Project (URAP) ozone climatology. The URAP correction to scattering ratio is typically 0.01 at 25km and 0.015 at 15km. Right; Altitude-time display of scattering ratio for 12 October, showing distinct layers. A time-invariant molecular density profile, obtained from the closest Aura/MLS measurements, has been used in calculating the scattering ratios. Data below 27km have been corrected for the attenuation effects of a mechanical shutter. Weak vertical features in the plot are due to fluctuations in the signal-to-noise ratio of the measurements. The ‘rising ledge’ feature in the scattering ratio history is discussed in the text.

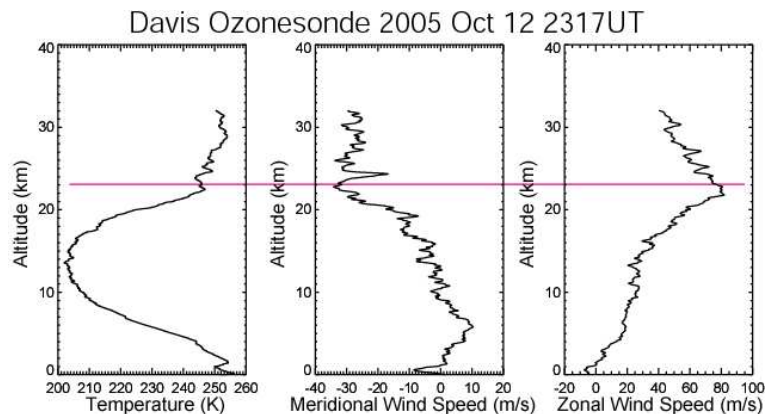


Fig 5. Profiles of temperature and wind speed obtained during the ozonesonde ascent. The horizontal red line marks the altitude of the narrow scattering ratio layer shown in figure 4. This altitude coincides with the peak wind speed. Perturbations in the profiles, particularly above 20km may be associated with gravity waves.

Discussion

In WMO (2005), evidence was presented for the association of the high ozone concentrations with a filament of ozone-rich air transported from tropical latitudes. Of

interest here is whether this air contained enhanced levels of aerosols, to produce the discrete layers in the lidar scattering.

The layer peaking near 23km altitude in figure 4 spans the altitude range of distinct features (the two lower 'ledges') in the ozone partial pressure profile of figure 1. The 'rising ledge' in the scattering ratio history highlighted in the right hand plot of figure 4 appears to lie at about 29km near 0100UT (13 October) when the ozonesonde measured a sharp transition in the ozone partial pressure (figure 1). On this basis, there appears to be an association of aerosols with increased ozone.

The Aura/MLS data for the mid-stratosphere have typical spatial resolution values of approximately 500km along-track, 5km cross-track and 3km vertically (Aura/MLS Level 2 Data Quality Document at <http://disc.gsfc.nasa.gov/aura/mls/documents/v1-5-report-29jul05b.pdf>). Because of the manner in which the lidar scattering ratio has been determined, the vertical structure and temporal changes shown in figure 4 conceivably reflect not only changes in the aerosol loading above the site, but also differences between the assumed and true molecular density profile (due for example, to small-scale temperature perturbations, the effects of which are resolved differently in the satellite and lidar data).

However, the cause of the discrete layer at 23km in figure 4 as due to a temperature perturbation is considered unlikely on the basis that the perturbation would represent a cool region with a temperature inversion on its low altitude side having a super-adiabatic lapse rate (approximately 13K/km as can be estimated from figure 3, compared with the adiabatic lapse rate for the stratosphere of ~10K/km). Such a layer in the stratosphere would be inherently unstable.

Consideration of trajectory analysis (figure 6) provides evidence that the unusual aerosol behaviour on 12 October was related to long-distance transport. In figure 6a, air arriving at Davis during the lidar observation of 11 October was confined to the polar region during the previous 10 days. Indeed, air below 25km altitude passed near the pole during the preceding 5 days and may have transported aerosols associated with the dissipation of Polar Stratospheric Clouds. For 12 October (figures 6b and 6c), air above 20km altitude was transported from well outside Antarctica (particularly for the ozonesonde flight). On 14 October (figure 6d), there was still a low-latitude connection above 30km and this may be associated with the tail in the scattering ratio profile above this height.

The temperature 'wave' between 20km and 35km apparent in figures 2 and 3 had a narrow latitudinal extent (a few hundred kilometres at 20hPa) as revealed by AIRS (figure 7). The temperature and wind shears near and within the layer are a potential source of gravity waves via baroclinic instability. The shears may also promote sorting of aerosol particles, and contribute to the layers apparent in the lidar scattering ratio analysis.

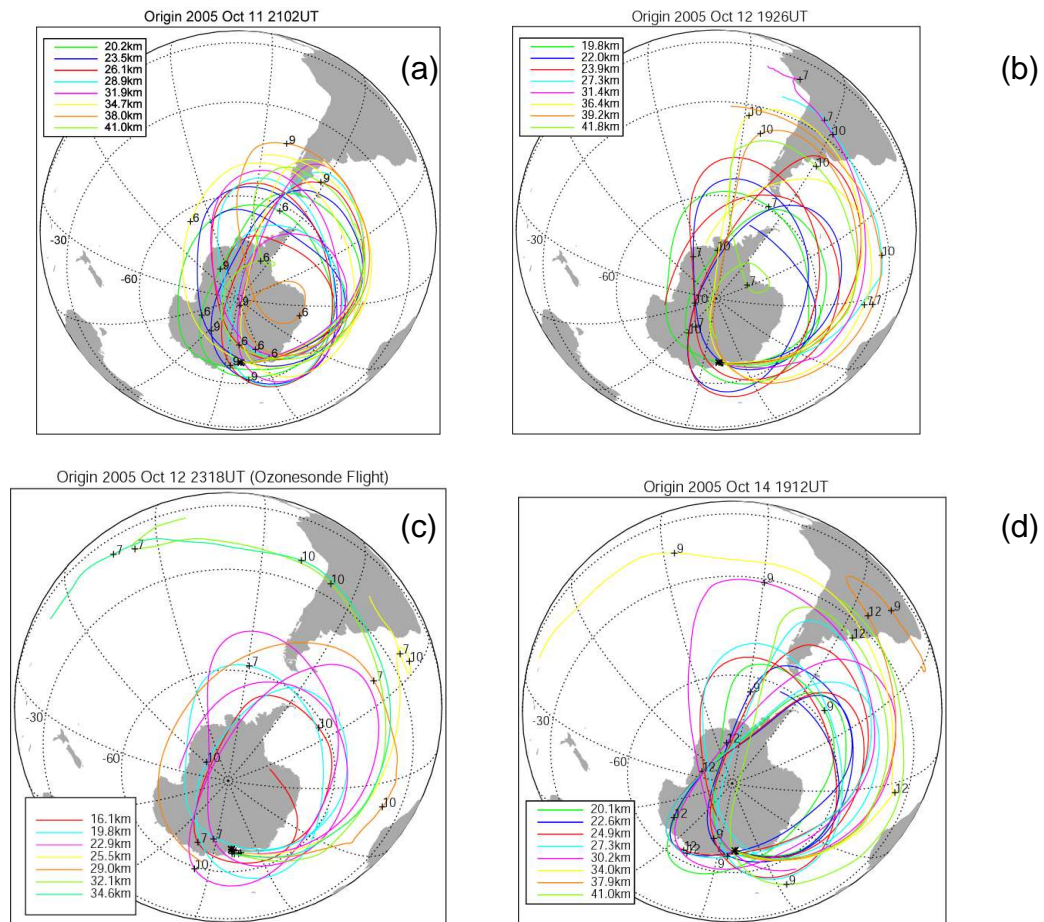


Fig 6. Backward trajectory analysis for air parcels originating at Davis, obtained from the NASA/Goddard Automailer (http://hyperion.gsfc.nasa.gov/Data_services/automailer), using Data Assimilation Office (DAO) meteorological model input. Fiducial marks show positions along the trajectory at 00UT on particular dates (day of October). The legend links each trajectory to its originating altitude. Above 20km altitude, the air sampled by the ozonesonde is modelled as originating well outside the Antarctic region. In particular, the two uppermost trajectories are placed at tropical latitudes about 5 days earlier.

Conclusions

Using ground-based and satellite measurements it has been shown that the observed enhanced ozone concentration over Davis on October were related to an episode of long-distance transport of low-latitude air to the edge of the Antarctic vortex. The air appeared confined to a relatively narrow filament containing air rich in ozone and aerosol, which was associated with large-scale wave activity.

Satellite temperature measurements, particularly from AIRS together with high resolution radiosonde data from the East Antarctic region should be investigated with a view to examining small-scale waves that may have been generated by shears associated with this feature. It is also of interest to examine any aerosol and trace gas measurements along the filament to gain insights into atmospheric transport, mixing and fractionation processes as well as to identify the origin of the aerosols.

Events such as this are relevant for the restoration of ozone levels during the spring break-up of the polar vortex and Antarctic ozone hole. Of further interest is examining the circumstances for their occurrence, and the mass of material that is transported.

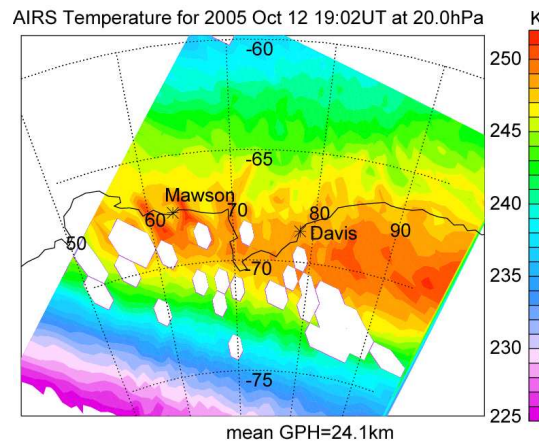


Fig 7. AIRS temperature map for the measurement granule in the vicinity of Davis closest to the ozonesonde and lidar observations. Data excluded on the basis of the data quality flags are shown as white pixels.

Acknowledgements

This paper was prepared under Australian Antarctic Science Project 737. Thanks are due to Andrew Cunningham (Australian Antarctic Division) for collecting the lidar data, to Mark Austin and Kevin Gunn (Australian Bureau of Meteorology; BoM) for launching the ozonesondes, and to Jim Easson (BoM) for processing the ozone data. The author acknowledges the following data sources; the British Atmospheric Data Centre (<http://badc.nerc.ac.uk>) for United Kingdom Meteorological Office Stratospheric Assimilated Data, BoM for radiosonde data, the NASA Goddard Spaceflight Center (<http://disc.gsfc.nasa.gov/Aura/MLS>) for Aura MLS data and trajectory analysis, the Goddard Distributed Active Archive Centre for AIRS data, the URAP data were obtained from the SPARC Data Center (<http://atmos.sparc.sunysb.edu>), and NASA Goddard Earth Observing System Data Assimilation System the for GEOS-4 data.

References

- Klekociuk, A.R, M.M. Lambert, R.A. Vincent, and A.J. Dowdy, 2003: First year of Rayleigh lidar measurements of middle atmosphere temperatures above Davis, Antarctica. *Advances in Space Research* 32, 771-776.
- WMO (World Meteorological Organisation), Antarctic ozone bulletin, 6, 2005 (<http://www.wmo.ch/web/arep/05/bulletin-6-2005.pdf>).

UV Index for Sun-Safety

L.Deschamps, P.Gies², L.Rikus, R.Dare³ and K.Strong⁴

Bureau of Meteorology Research Centre, Bureau of Meteorology

² Australian Radiation Protection and Nuclear Safety Agency, Australia

³ National, Meteorological and Oceanographic Centre, Bureau of Meteorology

⁴ Cancer Council Victoria, Australia

email: *L.Deschamps@bom.gov.au*

Abstract.

To help raise the awareness of the dangers of overexposure to UV radiation educational campaigns have been implemented along with UV measurements throughout Australia for over 20 years. In order to alert people of possible high levels of UV radiation, “UV Index” forecasts have been issued daily since 1997 as part of the weather report of the Bureau of Meteorology. To further promote sun protection the Sun Smart UV Alert was included recently in the weather report.

UV Index for Sun-Safety

The clear-sky local noon UV Index is calculated using the Bureau of Meteorology UV and Ozone forecasting system. The UV Index is the amount of UV radiation reaching the surface weighted by an average human skin spectral response to UV radiation. It is reported following the World Meteorological Organization international standard (Dixon et al., 2002) and presented in the table in Figure 1. More information can be found at <http://who.int/uv/en/>.

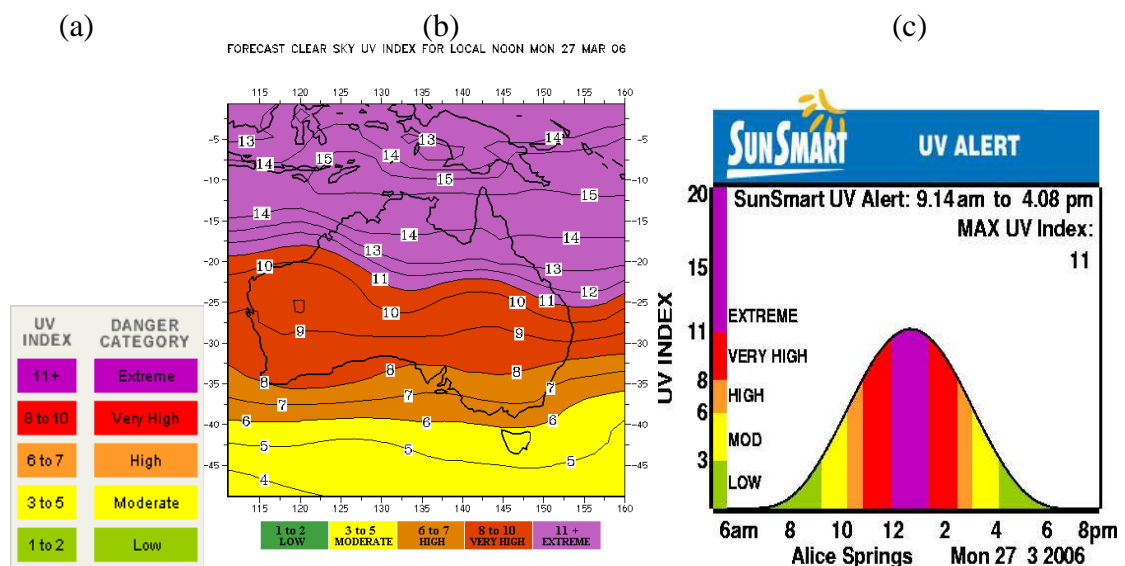


Figure 1. (a) The descriptive danger category table, (b) the Clear-sky UV Index forecast map for Australia for 27 March, 2006 and (c) the diurnal clear-sky UV Index forecast for Alice Springs with the SunSmart UV Alert (9:14am to 4:08pm) and the maximum UV Index for Alice Springs for 27 March 2006.

The effect of clouds is achieved by multiplying the clear-sky UV Index by a factor depending on the forecast cloud conditions. The UV Index is continuously validated against the Australian Radiation Protection and Nuclear Safety Agency measurements as part of an ongoing collaboration project (Gies et al., 2004, Lemus-Deschamps et al., 2004, Lemus-Deschamps et al, 2006). The UV Index is issued daily as a map for Australia and as a diurnal graph (Figure 1) and text for around 179 sites around Australia (<http://www.bom.gov.au/weather/national/charts/UV.shtml>) by the Bureau of Meteorology.

To further raise awareness of the levels of UV radiation the SunSmart UV Alert concept (<http://www.sunsmart.com.au>) has been included in the UV Index forecast graph (Figure 1) since December 2005. The SunSmart UV Alert has been added to encourage people to “be SunSmart” during the hours when the UV Index reaches 3 or above. The alert is issued daily by the Bureau of Meteorology as part of the UV report, when the UV Index forecast is 3 or more.

The Cancer Council Australia's key recommendations to be SunSmart are:

- 1) Seek shade.
- 2) Wear protective clothing that covers your arms and legs as well as your body.
- 3) Put on a broad-brimmed hat that shades your face and neck.
- 4) Wear wrap-around sunglasses.
- 5) Apply broad-spectrum SPF 30+ water resistant sunscreen every 2 hours. Sunscreen should not be used to extend the time you spend in the sun.

To further promote sun protection these recommendations and the graph in Figure 1. will be promoted by the SunSmart program to all schools and a number of other locations including outdoor workplaces around Australia. The idea is to encourage people as much as possible to “be SunSmart”.

Collaboration projects like the existing one between the Bureau of Meteorology, the Australian Radiation Protection and Nuclear Safety Agency and The Cancer Council are very important since Australia still has one of the highest rates of skin-cancer in the world.

Acknowledgements

We thank A. Hainsworth and his team from Weather and Ocean Services Policy Branch of the Bureau of Meteorology and L.Kuspira from The Cancer Council Victoria for all their support.

References

- Dixon, H., L. Lemus-Deschamps and P. Gies, 2002: Meteorology meets public health: UV forecasts and reports for sun safety. *Health Promotion, Journal of Australia*, **13**, 252, 2002.
- Gies P., C. Roy, S. Javorniczky, L. Lemus-Deschamps and C. Driscoll, 2004: Global Solar UV Index: Australian Measurements, Forecasts and Comparison with the UK. *Photochem.Photobiol*, **79**,32-39.
- Lemus-Deschamps, L., L. Rikus, S. Grainger, P. Gies, P., J. Sisson and Z. Li, 2004: UV Index and UV dose distributions for Australia (1997-2001). *Aust. Met. Mag.*, **53**, 239-250.
- Lemus-Deschamps, L., P. Gies, L. Rikus, K. Strong and H. Dixon, 2006: UV Index: Forecasts and Media Weather Reports. UV Radiation and its Effects, Workshop New Zealand, April 2006.